RECENT DEVELOPMENTS OF ECE DIAGNOSTICS AT JET

E. de la Luna[1], P. Blanchard[2], A. Bruschi[3], C. Cientioli[4], G. Conway[5], R. Felton[6], J. Fessey[6], C. Gowers[6], E. Joffrin[2], D.Mazon[2], A. Murari[7], S. Novak[3], M. Riva[4], A. Simonetto[3], C. Sozzi[3], J. Sanchez[1], M. Zerbini[4], and JET-EFDA contributors

[1]Asociacion EURATOM -CIEMAT para Fusion, CIEMAT, Spain,
[2]Association EURATOM-CEA, Cadarache, France
[3]IFP-CNR, Associazione EURATOM-ENEA-CNR sulla Fusione, Milano, Italy
[4]Associazione EURATOM-ENEA sulla Fusione, Frascati, Italy
[5]IPP- EURATOM Assoziation, Garching, Germany
[6]EURATOM -UKAEA Association, Culham Science Centre, Abingdon, UK
[7]Consorzio RFX, Associazione EURATOM -ENEA sulla Fusione, Padova, Italy

In this paper, the recent developments in the JET ECE diagnostic system will be described and illustrated with some recent results, with an emphasis on issues related with calibration stability, high-T_e plasmas and ITB studies. Some of these issues will be discussed in the context of ITER.

Introduction

Over the past few years, an important part of fusion research has been the development of advanced tokamak operation scenarios, with improved stability and confinement properties. This programme at JET is mainly focused on plasmas with internal transport barriers (ITB). The appearance of the ITB reduces the ion and electron heat (and/or particle) transport locally in the plasma core, which leads to a local increase of the pressure gradients, and depends strongly on the shape of the q-profile (see [1] for a review). The diagnosis of the plasma performance in these regimes needs detailed information regarding the spatial profiles of essential plasma parameters, such as the electron temperature, and its temporal evolution, which imposes extra demands on the required resolution. High spatial resolution is essential for resolving the steep temperature gradients (with typical scale lengths of only a few cm) characteristics of ITBs and the measurements must be time resolved because, in general, these regimes are not stationary. Thomson scattering measurements in JET [2], based on the light detection and ranging (LIDAR) technique, are problematic in this regard. The present JET Thomson scattering system provides one profile every 0.25 s and has a spatial resolution ~ 12 cm, which is insufficient for ITB studies. ECE diagnostics appear to be better suited to this purpose. They are able to provide time-resolved electron temperature profiles with high spatial and temporal resolution, and have played a fundamental role in the investigation and development of ITBs in JET.

In this paper we report on the major upgrade of the ECE diagnostics systems currently in progress at JET. Diagnostic developments include an upgrade of the multi-channel heterodyne radiometer [3], aimed at extending the radial region over which T_e measurement can be performed, and the installation of a new Michelson interferometer with fast scanning capability [4], to improve the frequency and temporal resolution of the multi-harmonic ECE measurements at JET. Moreover, a future extension of the ECE system, an *oblique* ECE diagnostic to measure the ECE spectra at different angles with respect to the normal to the magnetic field, is being developed in collaboration with groups of different EU national laboratories (CIEMAT, Spain and CNR-Milan, Italy). This diagnostic is expected to give valuable insight into the interpretation of ECE measurements in high T_e-plasmas and should be available for measurements once JET resumes operation in 2005.

The following article is divided as follows. We begin, in Sec. II, with an overview of the existing ECE diagnostics in JET, with special emphasis on the recent enhancements. A short survey of the recent results obtained with the ECE diagnostics in the last JET experimental campaigns will be reported in Section III, concentrating on their use for ITB studies. Future developments will be the subject of Sec IV. Finally we provide some concluding discussion.

2. ECE diagnostics in JET

In JET, two types of ECE instruments are routinely operated to provide electron temperature measurements: a Michelson interferometer and a heterodyne radiometer. Both systems have now been operational for some time. The Michelson interferometer [5] provides ECE spectra (X-mode) in the range 80-350 GHz, with moderate time (17 ms) and frequency resolution (10 GHz), whereas the multi-channel heterodyne radiometer gives reliable temperature measurements on a fast time scale (1 ms) with good spatial resolution (2-6 cm). Over the years the radiometer has been subjected to several enhancements that have been described in detail in earlier proceedings of this conference [6-7]. Here we give a brief overview of the instrument with details of the most recent upgrade [3]. The radiometer consists of six independent receivers, each of them having its own mixer and corresponding local oscillator, band-filter for proper sideband selection and IF (6 -18 GHz) amplifier chain. It covers the frequency range from 69 to 139 GHz. The previous set-up of the radiometer, limited by the number of channels (48 channels), covered a moderate spatial region of the T_e profile ($r/a \sim 0.2 - 1$) with high spectral resolution (frequency separation between channels ~ 0.5 GHz). To extend the use of the instrument further, the IF section has been modified to allow four adjacent mixers of the six available to be selected simultaneously (in the previous system only two mixers were selected). Since each mixer can be independently set to measure O-mode or X-mode (for 1st or 2nd harmonic ECE respectively), this allows a complete coverage of the plasma cross-section (limited to $R > 2.6$ m for X-mode polarization due to harmonic overlap) at all magnetic field values used in JET ($1.7\ T < B_T < 4\ T$). Note that the second harmonic (X-mode) is used for the lower fields and larger radii and the first harmonic (O-mode) for higher fields. To accommodate this extension of the radial coverage, without modifying the high spectral resolution of the original instrument, the number of channels has been doubled to 96 by adding two new IF filter banks up to a total of four. Each filter bank generates 24 channels in the conventional way, using power dividers and IF filters (with 250 MHz bandwidth) followed by Schottky-diode detectors and low noise video pre-amplifiers. New pre-amplifiers with a bandwidth of 1 MHz (110 kHz in the previous system) have been installed with the aim of increasing the usefulness of ECE signals for MHD and fluctuations studies. After the pre-amplifiers the signals are split into two parts, part going to the main amplifier (with remotely programmable gain and bandwidth) and the standard VME data acquisition board for T_e profile measurements and part going to a fast acquisition system. Note that the increase in the pre-amplifier bandwidth has no impact in the signal-to-noise ratio of the T_e profile data because the signals undergo additional filtering (adjustable between 1 and 5 kHz) in the main amplifier chain, which determines the final temporal resolution of the measurements.

2.1 Spatial resolution and accuracy of T_e profile measurements

An important consideration when using ECE as a T_e diagnostic is the spatial resolution that can be achieved. The spatial resolution of the observed emission along the line of sight is determined by the radial extent of the plasma emission volume, which depends on the optical depth of the plasma, and the bandwidth of the ECE receiver. For typical JET plasma conditions, the estimated radial resolution deduced from line broadening effects ranges from 2 cm at the outer edge to 4 cm at the magnetic axis [8] for the 2nd harmonic X-mode emission. The width of the emission layer becomes larger (3 - 6 cm) for the 1st harmonic O-mode due to its lower optical thickness. To estimate the overall spatial resolution, these values must be convolved with the bandwidth of the measurement system. In the case of the Michelson interferometer, Δf = 10 GHz, this results in ∼ 10 cm extra broadening, whereas for the radiometer, with Δf = 250 MHz, the effect is very small (< 1 cm). The last factor to be considered is the antenna pattern which broadens the volume contributing to the emission (~15 cm in the plasma centre) [9] and is the main limiting factor in the radial resolution of the current system.

Another key issue concerning ECE diagnostics is the accuracy of the absolute calibration. The Michelson interferometer is absolutely calibrated and the radiometer is cross-calibrated against the Michelson interferometer during the ohmic phase of the discharge. Recently, magnetic field ramp calibration shots have been analyzed in order to reduce the relative systematic errors in the absolute calibration [11]. By ramping the toroidal field (B_T) the resonance positions of the ECE moves through the spectrum. The shape of the T_e profile is kept nearly fixed by ramping the plasma current simultaneously such that the edge safety factor (q_a) remains constant. It is then possible to distinguish the errors in the calibration factors from real spectral features. This analysis [12] not only has significantly improved the smoothness and symmetry of the T_e profiles, but has also allowed us to re-examine the issue of the long-term calibration stability. The last absolute in-vessel calibration in JET was performed in May 1996. In general, good agreement is found between Thomson scattering and ECE temperature profiles for plasmas with low to moderate T_e (< 6 keV) [10], which gives us confidence in the Michelson interferometer calibration (uncertainty of ±10 %). On the other hand, the comparison of the corrected calibration factors obtained using data collected during B_T-ramp discharges since 1996 has shown that the differences in the system response over a period of 8 years are less than 5%. It is therefore concluded that it is possible to maintain a stable and reliable calibration over long periods of time. This result is of major importance for the application of ECE techniques on ITER, which will need low-maintenance systems.

3. Experimental results

The ECE systems are used routinely in the study of a wide range of plasma phenomena in JET. In this section we present several examples of recently obtained results that characterize the performance of the ECE diagnostics, with an emphasis on high-T_e plasma and ITB measurements.

3.1. Internal transport barriers measurements

The radiometer has played a key role in the investigation of ITBs in JET due to its excellent accuracy and high spatial resolution that enables this system to resolve the steep temperature gradients formed at the plasma core during ITBs with good temporal resolution. The basic scenario for the generation of ITBs in JET consists on applying lower hybrid current drive (LHCD) or ion cyclotron resonance heating (ICRH) during the initial current ramp-up phase of the discharge to form a q-profile with reversed or weak magnetic shear. Subsequently the ITB is established during the main heating phase, mainly a combination of neutral beam injection (NBI) and ICRH [13-14]. An example of a high density ITB [14] seen on the T_e profile is shown in figure 1. In this case, a set of pellets is injected just before the start of the main heating phase (B_0 = 3.2 T, P_{NBI} = 8 MW, P_{ICRH} = 6 MW) and a strong ITB is formed with central density close to the Greenwald limit ($n_e(0) = 6\times10^{19}$ m^{-3}) and similar electron and ion temperature. The ITB location can be clearly inferred from the discontinuity in the temperature gradient determined from the ECE profile, but it is not properly resolved by the Thomson scattering (TS) diagnostic due to its insufficient spatial resolution. It is also observed that the T_e profile is very flat in the central region, which indicates very poor confinement. This is attributed to the existence of a 'current hole', a region with zero current density [15]. This figure illustrates the extended radial coverage of the upgraded radiometer (r/a ~ 0.2 – 1 for the previous system) that allows the simultaneous observation of both high and low field side internal transport barriers. To compare the profiles measured by the different diagnostics, which have different lines of sight, the radial positions are mapped from their sightlines (and B space in the case of ECE) onto the magnetic axis using the EFIT equilibrium reconstruction code. In most cases, the plasma centre is not accessible for the radiometer, whose line sight is typically located below the magnetic axis. Generally, the mapping of the ECE measurements does not include the correction due to the relativistic broadening of the emission (inward shift of the emission origin). This correction is usually small but increases with the T_e and can have a significant effect in high T_e-plasmas. This results in a systematic error in the ITB position ~ 1- 3 cm [8].

Figure 2 shows another example of electron ITBs, in this case obtained during the low power LHCD prelude phase in the presence of strong negative central shear. LH waves not only drive off-axis current but also heat the electrons and temperature in excess of 10 keV can be obtained [12]. The plasma density is typically low during this phase. Steep temperature gradients are clearly recognized in the ECE profile indicating the existence of an ITB. This scenario tends to generate narrow ITBs. Here the enhanced gradient region is seen in the region $r/a < 0.2$.

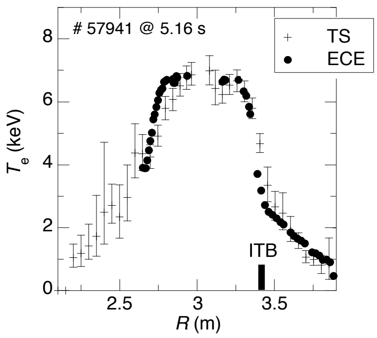

Fig.1. *T_e profiles as measured by ECE and Thomson scattering for a high density ITB discharge. The extended radial coverage of the upgraded radiometer allows the simultaneous observation of both high and low field side ITBs.*

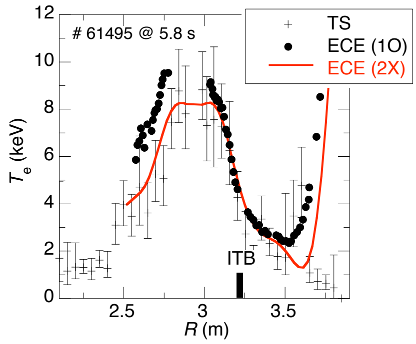

Fig. 2. ITB obtained during LHCD experiments (B_0=3.46 T, P_{LH} = 3 MW, $n_e(0)$ = 1.5×10^{19} m^{-3}). Shown are the T_e profiles measured by the Thomson scattering diagnostic, the radiometer (1st harmonic, O-mode) and the Michelson interferometer (2nd harmonic, X-mode).

One concern in LHCD experiments is whether the radiation temperature measured by ECE is effectively the same as the bulk temperature. ECE measurements are clearly affected by supra-thermals in a narrow region near the plasma edge (lowest optical depth) due to downshifted non-thermal emission (see figure 2). On the other hand, at low electron densities, 3rd harmonic (2nd harmonic for O-mode) downshifted non-thermal emission can contribute significantly to the radiation temperature measured in the plasma core. A number of consistency checks can be performed to determine the thermal character of the emission. First, for an optically thick plasma the T_e values measured by ECE must agree, within the error bars, with the independently calibrated Thomson scattering diagnostic. Second, the emission at the low and high field side can be compared. If both emissions show similar intensity, there is a strong indication that the emission is thermal. This seems to be the case of the T_e deduced from the 2nd harmonic X-mode emission measured by the Michelson interferometer. However, a disagreement is observed between the radiometer and Thomson scattering data for R < 3 m. It has to be mentioned that for this experiment (with B_0 = 3.46 T) the radiometer is set to measure the 1st harmonic O-mode. This implies that the radiometer data might be partially over-estimated because no correction in the calibration has been made to account for the lower optical thickness of the O-mode radiation (simulations show that for ohmic plasmas $T_{rad}^{1O} / T_{rad}^{2X} \approx 0.95$ in the plasma high field side). However, it should be noted, that the observed discrepancy between the $T_{\rm rad}$ measured by the Michelson interferometer and the radiometer for R < 3 m can also be influenced by the different sensitivity of the two harmonics to supra-thermal electrons, as O-mode radiation intensity depends on both $v_{||}$ and $v_{\perp}$, whereas the X-mode only depends on $v_{\perp}$ (where $v_{||}$ and $v_{\perp}$ are the parallel and perpendicular velocity of the resonant electrons respectively). The origin of this discrepancy is still under investigation.

3.2. T_e measurements in high power auxiliary (ICRH+NBI) heated plasmas

With the advent of improved confinement regimes, plasmas with central temperatures well in excess of 7 keV have been obtained in JET, generally by using a combination of neutral beam injection and ion cyclotron heating. It has been found that for these high-T_e plasmas a systematic disagreement appears between the central temperatures measured by ECE and Thomson scattering [10]. The temperature measured by ECE can be up to 15% higher than the one measured by Thomson scattering (see Fig. 3). The peculiarity of the observed discrepancy is that it appears in a region where the optical thickness of the plasma is higher. Similar effect was observed on TFTR [17] and also during the alpha heating experiments carried out in JET in 1997 and has remained unexplained so far. Thomson scattering measures the velocity distribution of the bulk electrons, but ECE emission is blackbody ($T_{\rm rad} = T_e$) only if the distribution is Maxwellian. Therefore, discrepancies between ECE and Thomson scattering temperature profiles can be used for diagnostic purposes as a tool to identify the existence of non-Maxwellian features in the electron distribution function [19]. Moreover, ECE spectra measured in those plasma conditions are also inconsistent with the electron bulk distribution being Maxwellian in the plasma core, as can be seen in Fig. 4, where measured and simulated ECE spectra are compared. The 3rd harmonic emission is optically thick in these high-T_e plasmas

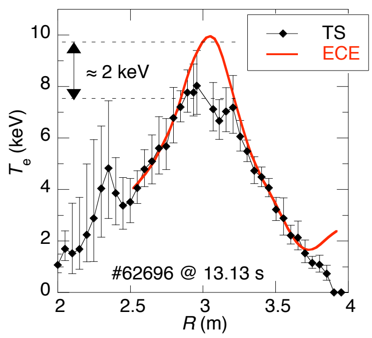

Fig. 3. *T_e profile measured by ECE (Michelson interferometer) and Thomson scattering for a plasma heated by ICRH + NBI (B_0 = 3.2 T, P_{NBI} = 8 MW, P_{ICRH} = 8 MW, P_{LH} = 0.5 MW).*

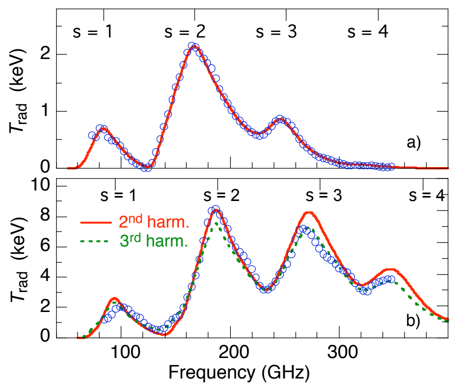

Fig. 4. *X-mode ECE spectra measured with the Michelson interferometer (symbols) and the corresponding simulated spectra assuming a Maxwellian distribution function obtained by fitting the 2nd harmonic (full lines) or the 3rd harmonic (dashed lines). (a) Ohmic case (B_0=3.04 T, $n_e(0)$=1.98×10^{19} m^{-3}), (b) combined ICRH + NBI heating (P_{NBI} = 15.7 MW, P_{ICRH} = 5 MW, B_0 = 3.4 T, $n_e(0)$ = 3.3×10^{19} m^{-3}) (from. Ref. [10])*

and therefore provides an independent measurement of the bulk electron temperature but related to electrons with higher energy [18]. However, as can be seen in Fig. 4(b), the central temperature deduced from the 3rd harmonic is lower than the one deduced from the 2nd harmonic. The agreement found between the simulated and measured spectra for thermal plasma conditions (see Fig. 4(a)) gives us confidence that the difference observed is not due to any calibration error. All of these experimental results appear to be consistent with the existence of a deformation of the bulk of the electron distribution function at r/a < 0.35, sharply localized at $u/u_{\rm th}$ < 1.5 ($u_{\rm th}$ is the thermal momentum) [10]. Similar effects have been observed in FTU during high power electron cyclotron resonance heating (ECRH) experiments [19,20]. The detailed understanding of this intriguing result is crucial when considering the application of the ECE diagnostics in ITER, where the range of electron temperatures presently expected is about a factor of two bigger than those of the existing tokamaks. To investigate this problem an *oblique* ECE diagnostic, based on the observation of the emission at different angles with respect to the magnetic field, has been proposed and will be discussed in section 4.

3.3 Real-time control experiments

In the last 4 years, JET has developed an ambitious program to implement a real time control system [21], which integrates many different diagnostics, with the objective of achieving and controlling steady state ITB regimes. In JET it was found that the appearance of an ITB can be detected by using the criterion $\rho_T^* = \rho_s / L_T \geq 1.4 \times 10^{-2}$ [22], where ρ_s is the Larmor radius at the sound speed, $\rho_s = c_s/\omega_{ci}$, c_s is the ion sound speed, ω_{ci} is the ion cyclotron frequency and L_T is the temperature gradient scale length, $L_T = -T/(\mathrm{d}T/\mathrm{d}r)$. The maximum value of ρ_T^* and the radii where the mentioned criterion is satisfied determine the strength and the location of the ITB respectively. Real time experiments require an online evaluation of the ITB criterion, which for electron transport barriers is inferred from the ECE radiometer data. The procedure for calculating $\rho_{T_e}^*$ in the

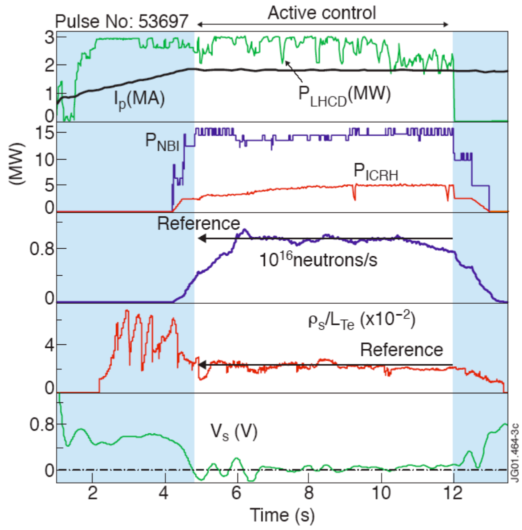

Fig. 5. *Time evolution of a JET discharge (1.8 MA, 3.4 T) with an ITB and full non-inductive current ($V_{loop}\approx 0$) using feedback control of the neutron rate by NBI and the ITB strength (ρ_{Te}*)(from Ref. [23])*

real-time system for control applications is as follows: the measured ECE signals are low pass filtered (200 Hz) and sent to dedicated ADCs that provides ECE raw data (96 channels) at a frequency of 100 Hz. The signals are calibrated using the calibration factors of a previously selected reference discharge. The calibration factors, deduced by cross-calibration with the Michelson interferometer, are mainly sensitive to the toroidal field value as this parameter determines which is the best combination of mixers and polarizations for the maximum available radial coverage. Non-thermal features in the ECE data, such as downshifted emission at the plasma edge during LH heating or spikes of intense radiation observed during ELMs, are automatically excluded from the calculation of L_T.

Active control of the ITB has been successfully demonstrated in JET. Figure 5 shows an example in which feedback control on the neutron rate and the electron temperature profile was implemented by using NBI and ICRH heating respectively [23]. The improved plasma performance is, at present, transient, and experiments are now being design to extend this regime of operation to steady state by controlling the pressure and current profiles simultaneously [24].

4. Future developments

An *oblique* ECE system is now being developed at JET. This challenging diagnostic will use the emission collected at an angle with respect to the normal to the magnetic field ($\phi = 0^\circ$, for standard ECE measurements) and it is proposed as a way of studying the bulk of the distribution function with good spatial and energy resolution. Comprehensive reviews of the diagnostic potential of the oblique ECE measurements already exist in the literature [19,25,26]. Detailed calculations have confirmed the applicability of this technique for JET plasma parameters provided the observation angle is not too large ($\phi < 20^\circ$) [10]. Modelling of the LH heating and current drive could also profit from this kind of measurements, however the angular range available in JET would not allow us to fully investigate the high-energy tail generated during LHCD experiments. The diagnostic can be conceptually divided into two units, the antenna and the detection system. It will use two of the six new waveguides, arranged in a cluster of 3 × 2 (horizontal × vertical), that will be installed within the framework of the new Microwave Access project [27] and basically consist of an open-ended circular waveguide whose beam is tilted in toroidal direction (ϕ~ 10˚ and 20˚) by using the combinations of fixed mirrors shown schematically in Fig. 6 [28]. The last mirror is elliptical in order to control the size of the final beam. The detection system will be a new Michelson interferometer with fast scanning capability that has already been installed at JET and is currently being commissioned. It uses a single, large-size rotating modulator, based on the technique successfully developed and tested on FTU [29]. This will result in a significant increase in the spectral (6 GHz) and temporal (up to 5 ms, for a single ECE spectrum) resolution of the ECE spectra measurements. The instrument is going to be upgraded to increase the number of channels up to 6 (originally designed for 4 channels). This will allow the simultaneous measurement of the ECE spectrum at different angles (including ϕ ~ 0˚) with different polarizations (O- and X-mode).

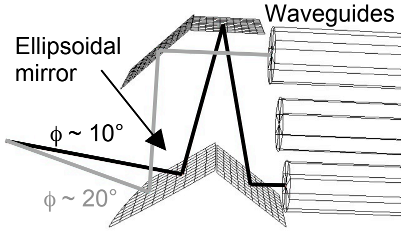

Fig. 6. *Conceptual design (top view) of the oblique antenna for JET. It provides two oblique views (ϕ~ 10˚ and 20˚) by using three plane mirrors and an elliptical one that is shared by the two viewing lines. The central waveguide will be used for reflectometry.*

5. Conclusions

JET ECE diagnostics have performed reliably as a standard electron temperature diagnostics and have played a key role in the understanding and development of advanced operation scenarios in JET. One of the most fruitful applications of ECE measurements has been the use of T_e profile data for real time control of the ITB formation. This has proven to be very helpful to improving the stability and reliability of this operation mode. Furthermore, the operating experience obtained at JET with the Michelson interferometer, which has been successfully used for several years, has demonstrated a long-term stability in its absolute calibration. This information is particularly relevant for next generation of fusion devices, in which long-term maintenance-free operation is required.

A substantial enhancement of the ECE diagnostic system is currently under progress in JET. Taken together, these enhancements, the 96-channels radiometer, the new Michelson interferometer with improved temporal and frequency resolution and the new *oblique* ECE antenna provide JET with one of the most comprehensive ECE systems thus far in operation in a fusion device. The different instruments have different advantages and will be used complementary. The interest in measuring the ECE spectra in a wide frequency range goes beyond the determination of the temperature profile. The comparison of the peak radiation temperatures at different optically thick harmonics provides a very useful tool for a cross-check of temperature measurements in case of poor agreement between the usual T_e diagnostics. These comparisons in JET have highlighted a systematic disagreement between Thomson scattering and ECE temperatures in high-T_e plasmas. The analysis carried out at JET seems to indicate that the assumption of a Maxwellian bulk may not be necessarily true in the presence of strong auxiliary heating, contrary to what it is usually assumed. The *oblique* ECE diagnostic proposed for JET will provide a unique opportunity to explore the physics of high-T_e plasmas under conditions approaching those relevant to a tokamak reactor and can contribute significantly to improve the ability to interpret accurately ECE measurements in ITER.

Acknowledgements

The authors would like to acknowledge R. Prentice, D. Bartlett, L. Porte and H. Oosterbeek for their contributions to the design and development of the JET ECE diagnostics. This work has been conducted under the European Fusion Development Agreement.

References

[1] R. Wolf, Plasma Phys. and Control. Fusion **45** (2003) R1
[2] C. Gowers *et al.*, Rev. Sci. Instrum. **66**, 471 (1995)
[3] E. de la Luna *et al.*, Proc. 15th High Temperature Plasma Diagnostics, San Diego (2004)
[4] M. Zerbini *et al.*, Proc. 15th High Temperature Plasma Diagnostics, San Diego (2004)
[5] A. E. Costley *et al.*, Proc. of the 5th Joint Workshop on ECE and ECRH, San Diego (1985)
[6] D. Bartlett *et al*., Proc. 8th International Workshop on ECE and ECRH, GutIsing, (1992)
[7] D. Bartlett *et al*., Proc. 9th International Workshop on ECE and ECRH, Borrego Springs (1995)
[8] V. Tribaldos, EFDA-JET Report, EFD-P (01) 44 (2001)
[9] N. A. Salmon *et al.*, Proc. 6th Joint Workshop on ECE and ECRH, Oxford, UK (1987)
[10] E. de la Luna *et al.*, Rev. Sci. Instrum. **74** (2003) 1414
[11] H. Bindslev and D. Bartlett. JET Report No. R(88) 04
[12] P. Blanchard *et al.*, Proc. 15th High Temperature Plasma Diagnostics, San Diego (2004)
[13] C. Challis *et al.*, Plasma Phys. and Controlled Fusion **43** (2001) 861
[14] X. Litaudon *et al.*, Nuclear Fusion **43** (2003) 565
[15] D. Frigione *et al*., Proc. 30th EPS Conf. on Contr. Fusion and Plasma Phys., St. Petersburg, (2003)
[16] N. Hawkes *et al.*, Phys. Rev. Letters **87** (2001) 115001
[17] G. Taylor *et al.*, Proc. 9th Joint Workshop on ECE and ECRH, Borrego Spring (1995) 485
[18] I. Fidone *et al.*, Phys. Plasmas **3** (1996) 2331
[19] V. Krivenski. Fusion Engineering and Design **53** (2001) 23
[20] E. de la Luna *et al.*, Proc. 12th Joint Workshop on ECE and ECRH, Aix-en-Provence (2002)
[21] E. Joffrin *et al.*, Plasma Phys. and Control. Fusion **45** (2003) A367
[22] G. Tresset, *et al.*, Nuclear Fusion **42** (2002) 520
[23] D. Mazon *et al.*, Plasma Phys. and Controlled Fusion **44** (2002) 1087
[24] D. Mazon *et al.*, Proc. 30th EPS Conf. on Contr. Fusion and Plasma Phys., London (2004)
[25] V. Tribaldos et al., Proc. 8th Joint Workshop on ECE and ECRH, GutIsing (1992)
[26] S. Preische *et al.*, Rev. Sci. Instrum. **68** (1997) 409
[27] L. Cupido *et al.*, Proc. 23rd Symposium on Fusion Technology, Venice (2004)
[28] C. Sozzi *et al.*, Proc. 23rd Symposium on Fusion Technology, Venice (2004)
[29] P. Buratti and M. Zerbini. Rev. Sci. Instrum. **66** (1995) 4208